Cell

Molecular Basis for Target RNA Recognition and Cleavage by Human RISC

Stefan Ludwig Ameres,[1] Javier Martinez,[2,*] and Renée Schroeder[1,*]
[1] Max F. Perutz Laboratories, University of Vienna, Dr.-Bohr-Gasse 9/5, A-1030 Vienna, Austria
[2] Institute of Molecular Biotechnology of the Austrian Academy of Sciences, IMBA, Dr.-Bohr-Gasse 3-5, A-1030 Vienna, Austria
*Correspondence: javier.martinez@imba.oeaw.ac.at (J.M.), renee.schroeder@univie.ac.at (R.S.)
DOI 10.1016/j.cell.2007.04.037

SUMMARY

The RNA-Induced Silencing Complex (RISC) is a ribonucleoprotein particle composed of a single-stranded short interfering RNA (siRNA) and an endonucleolytically active Argonaute protein, capable of cleaving mRNAs complementary to the siRNA. The mechanism by which RISC cleaves a target RNA is well understood, however it remains enigmatic how RISC finds its target RNA. Here, we show, both in vitro and in vivo, that the accessibility of the target site correlates directly with the efficiency of cleavage, demonstrating that RISC is unable to unfold structured RNA. In the course of target recognition, RISC transiently contacts single-stranded RNA nonspecifically and promotes siRNA-target RNA annealing. Furthermore, the 5′ part of the siRNA within RISC creates a thermodynamic threshold that determines the stable association of RISC and the target RNA. We therefore provide mechanistic insights by revealing features of RISC and target RNAs that are crucial to achieve efficiency and specificity in RNA interference.

INTRODUCTION

RNA interference (RNAi) is a homology-dependent gene silencing process, which occurs in a variety of evolutionary diverse organisms (Filipowicz, 2005; Fire et al., 1998; Napoli et al., 1990; Tomari and Zamore, 2005). The RNAi pathway is triggered by exogenous or endogenous, long double-stranded RNA molecules (dsRNA), which are processed by RNase III-like enzymes, resulting in the formation of ~21 nucleotide (nt) short dsRNAs (Bernstein et al., 2001; Elbashir et al., 2001b; Ketting et al., 2001; Knight and Bass, 2001; Lee et al., 2003). These short interfering RNAs (siRNAs) or micro RNAs (miRNAs) are then transferred to the RNAi effector complex, the RNA-Induced Silencing Complex (RISC) (Hammond et al., 2000). RISC assembles on one of the two strands of an siRNA or miRNA duplex and activation of RISC requires the removal of the passenger strand (Khvorova et al., 2003; Leuschner et al., 2006; Matranga et al., 2005; Miyoshi et al., 2005; Rand et al., 2005; Schwarz et al., 2003). Activated RISC is a ribonucleoprotein complex and consists in its core of an Argonaute protein and a single-stranded siRNA or miRNA, which acts as a guide to target complementary sequences within mRNAs (Elbashir et al., 2001b; Liu et al., 2004; Meister et al., 2004). Depending on both the nature of the Argonaute protein and the degree of complementarity between the siRNA and the target sequence, association of human RISC with mRNAs can result in multiple silencing modes including endonucleolytic cleavage, translational repression, deadenylation and sequestration to P-body compartments (Valencia-Sanchez et al., 2006).

The human genome encodes four Argonaute proteins (hAgo1–4) that are ubiquitously expressed (Sasaki et al., 2003). Of these, only hAgo2 is endonucleolytically active (Liu et al., 2004; Meister et al., 2004; Rivas et al., 2005). Cleavage catalysis is mediated by the PIWI domain of hAgo2, is Mg^{2+}-dependent and occurs specifically 10 nt from the 5′-end of the siRNA, leaving the siRNA intact for another round of cleavage (Elbashir et al., 2001c; Hutvagner and Zamore, 2002; Liu et al., 2004; Martinez and Tuschl, 2004; Rivas et al., 2005; Schwarz et al., 2004; Song et al., 2004). The complete protein composition of RISC is not entirely clear and the reported sizes of this complex vary from ~160 kDa (minimal RISC) to ~80 S (holo-RISC) (Hammond et al., 2001; Hutvagner and Zamore, 2002; Martinez et al., 2002; Nykanen et al., 2001; Pham et al., 2004). However, the good agreement of kinetic data derived from different sources of RISC, including *Drosophila* embryo extracts, affinity-purified human RISC or recombinantly expressed hAgo2 in complex with a single-stranded siRNA, suggests that a minimal activated RISC, consisting solely of hAgo2 and the siRNA guide strand, is not assisted by other proteins that remodel or activate the complex for substrate binding and cleavage (Haley and Zamore, 2004; Martinez and Tuschl, 2004; Rivas et al., 2005). Although the mechanism of RISC-mediated target RNA cleavage catalysis has been analyzed in detail (Haley and Zamore, 2004; Liu et al., 2004; Ma et al., 2005; Martinez and Tuschl, 2004; Meister et al., 2004; Schwarz et al., 2004; Song et al., 2004),

several questions concerning individual steps in the process of RISC-mediated target RNA recognition remain unanswered.

For example, how can RISC efficiently find its target? It has been suggested that RISC might utilize the translation machinery to scan mRNAs, as RISC was found to be associated with ribosomal factors (Caudy et al., 2003, 2002; Hammond et al., 2001; Ishizuka et al., 2002; Pham et al., 2004). However, just recently two groups confirmed earlier indications that translation is not required for efficient RNAi (Gu and Rossi, 2005; Sen et al., 2005; Zamore et al., 2000). Nevertheless, it is evident that RISC-mediated siRNA-target interaction is more complex than simple nucleic acid hybridization and that presumably some factor within RISC facilitates target recognition via an as yet unknown mechanism (Hutvagner et al., 2004).

Another area of investigation is whether the structure of target RNAs influences RNAi efficiency. Data arguing for and against target site accessibility have been reported (Boese et al., 2005; Heale et al., 2005; Long et al., 2007; Luo and Chang, 2004; Overhoff et al., 2005; Schubert et al., 2005). However, the major drawback for such studies was the lack of tools to accurately and reliably predict secondary structures within long RNAs, like mRNAs. Probably the strongest evidence for target site accessibility effects comes from an elegant but indirect in vitro approach in which folding of target RNAs was artificially blocked (Brown et al., 2005). Despite the existing evidence for a role of target mRNA structure in RNAi efficiency, the mechanistic basis for this effect is unknown. It is still unclear how minor changes in the sequence of an siRNA can dramatically impair RISC cleavage activity (Boese et al., 2005). Multiple steps in the RNAi pathway might be affected by changes in the sequence composition including RISC assembly, siRNA strand selection and target site accessibility.

Here, we used a minimal system to investigate how the secondary structure of target RNAs influences target recognition and cleavage by human RISC, independent of upstream events in the RNAi pathway, e.g., RISC-assembly. We found that RISC is incapable of unfolding target RNA secondary structures. As a consequence, cleavage is highly dependent on target site accessibility. We also identified minimal contacts required for efficient cleavage of the RNA target and enzyme turnover. High accessibility of the target site can be sensed by an intrinsic, nonspecific affinity of RISC for single-stranded RNA and interestingly, RISC-mediated target cleavage, even in a reconstituted in vitro system, is far more efficient than simple nucleic-acid hybridization.

RESULTS

To characterize how different target RNA structures influence RISC-mediated target recognition and cleavage, we compared cleavage rates of ~50 nucleotide (nt) long, in vitro transcribed and ^{32}P-cap labeled RNAs, containing a 21 nt target site derived from the sequence of the firefly luciferase (Elbashir et al., 2001a; Martinez et al., 2002; Schwarz et al., 2004). Changes in the sequence composition of the target RNAs outside of the 21 nt target site resulted in different secondary structures, which were determined in silico, using the mfold algorithm (Mathews et al., 1999; Zuker, 2003). Unimolecular structure formation was confirmed experimentally by performing UV melting analysis (data not shown). The limited length of the target RNAs facilitates the design of defined structures, which in case of long RNAs, like mRNAs, is not reliable.

To assess the influence of different RNA structures on RISC-mediated cleavage we performed in vitro cleavage assays using affinity-purified human RISC (Martinez et al., 2002). As the sequence of both, the target site and the siRNA within RISC, remains the same throughout the study, any changes in cleavage rates can be ascribed solely to the influence of target RNA structures. Importantly, this system is independent of any upstream event in the RNAi pathway including RISC assembly or siRNA strand selection.

Target Site Accessibility Determines RISC-Mediated Cleavage In Vitro and In Vivo

To analyze how target RNA structures influence cleavage by RISC, we designed RNAs with a stepwise-reduced accessibility of the target sequence due to an increase in secondary structure stability (Figure 1A). In a time course, decrease in accessibility led to reduction in cleavage efficiency (Figure 1B). Mod33, in which the target sequence is completely blocked due to base pairing, could no longer be cleaved (Figure 1B). Plotting the normalized cleavage efficiencies of the different target RNAs, as determined by the initial velocity of cleavage (Figure 1B), against the free energy value of the corresponding secondary structure (–ΔG; Figure 1A), revealed a linear correlation between increase in secondary structure stability and decrease in cleavage efficiency (Figure 1C). Therefore we conclude that secondary structures, directly blocking the accessibility of the target site, reduce RISC-mediated cleavage efficiency in a manner that is dependent on secondary structure stability. The fact that cleavage is sensitive to secondary structures with low stability (e.g., $\Delta G = -5.7$ kcal/mol; Figures 1A–1C), indicates that RISC does not display RNA unfolding activity. However, although the initial velocity of cleavage is clearly affected by reduced target site accessibility, we find that a significant impairment in target cleavage at late time points (e.g., after over night incubation) is restricted to secondary structures with a stability of at least −18 kcal/mol or −23 kcal/mol (Figure S1 in the Supplemental Data available with this article online), implying that cleavage of even severely structured RNAs would finally reach the maximum observed with less structured target RNAs. Therefore we asked to what extent secondary structures affect RNAi knockdown experiments in cell culture.

A subset of the target RNAs shown in Figure 1A was cloned into the 3′-UTR of Renilla luciferase under the

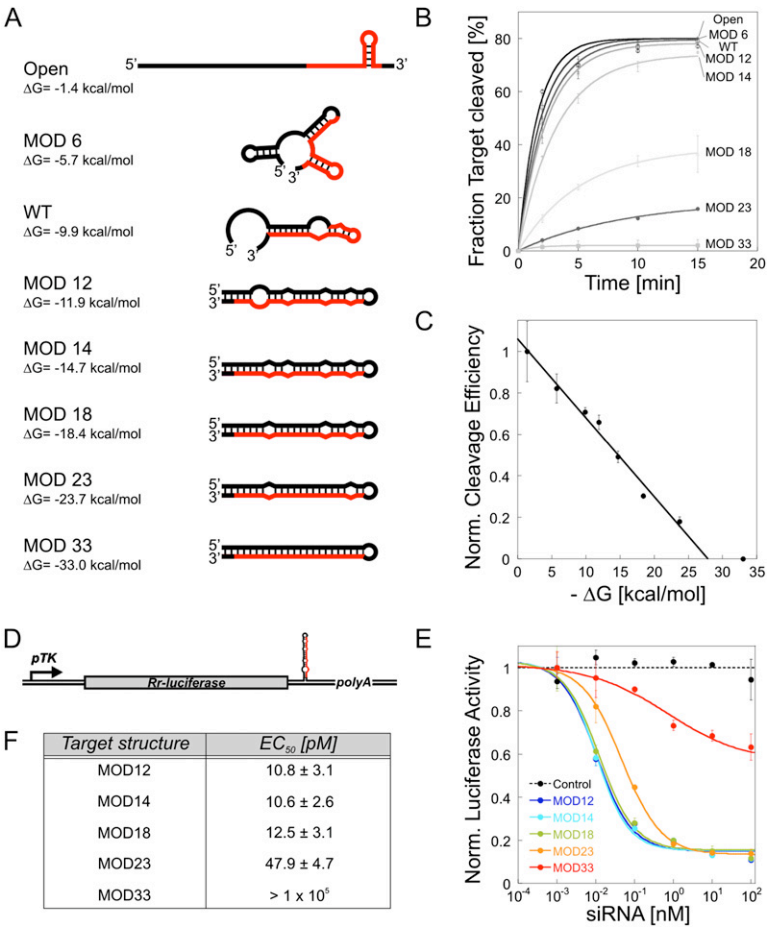

F

Target structure	EC_{50} [pM]
MOD12	10.8 ± 3.1
MOD14	10.6 ± 2.6
MOD18	12.5 ± 3.1
MOD23	47.9 ± 4.7
MOD33	> 1 x 10^5

Figure 1. The Accessibility of the Target Site Determines RISC-Mediated Cleavage In Vitro and In Vivo

(A) Schematic overview of target RNAs, which fold into distinct secondary structures. The corresponding free energy value (ΔG) is indicated. The target site is shown in red and is identical in all target RNAs.

(B) Quantification of the in vitro cleavage assays using affinity-purified human RISC and the indicated target RNAs. Data are represented as mean ± SD

(C) Correlation between target RNA secondary structure stability (ΔG) and cleavage efficiency. The normalized cleavage efficiency was determined from the initial velocity of the cleavage reaction shown in (B). Cleavage efficiency of target RNA "Open" was set as 1.

(D) A subset of target RNAs shown in (A) was cloned into the 3′-UTR of *Renilla reniformis* (Rr) Luciferase which is under the control of a constitutively active thymidine kinase (TK) promoter.

(E) HeLa cells were transfected with the indicated reporter constructs and increasing amounts of siRNA. 24 h post transfection, luciferase activity was determined. Luciferase activity after transfection of the vector without siRNA was set as 1. Data are represented as mean ± SD

(F) The siRNA concentration required for half maximal reduction of luciferase expression (EC_{50}) was calculated for each dataset shown in (E).

control of a TK promoter to achieve constitutive levels of reporter expression (Figure 1D). HeLa cells were transiently transfected with the respective reporter constructs and increasing amounts of siRNA duplex. The sequences of the target site and the siRNA duplex were identical in every assay, excluding upstream effects on RNAi efficiency. After 24h, which is the shortest incubation time in standard RNAi knockdown experiments, the cells were lysed, Renilla luciferase activity was determined and normalized for transfection efficiency and protein levels (Figure 1E). Comparison of the effective siRNA concentration, which led to 50% reduction in luciferase expression (EC_{50}) showed that the knockdown efficiency was not changed for secondary structures with a stability of up to −18 kcal/mol (EC_{50} = ~11 pM; Figure 1F). Further increase in secondary structure stability to −23 kcal/mol resulted in 4 fold (EC_{50} = ~48 pM) and to −33 kcal/mol in over 10,000 fold (EC_{50} > 100 nM) increase in EC_{50} values. Therefore secondary structures can severely affect RNAi knockdown efficiency in vivo, and a significant impact on RNAi knockdown is predicted to appear in the range of ΔG = −23 to −33 kcal/mol, at least with an siRNA that is effectively assembled into RISC. Furthermore, these results are remarkably similar to the impairment in cleavage observed under in vitro conditions using affinity-purified RISC (Figure S1), suggesting that target recognition and cleavage is not supported by auxiliary factors in a potential holo-RISC complex in human cells.

Minimal Target Site Accessibility for Efficient Cleavage

To assess the influence of partially blocked target sites on target recognition and cleavage by RISC, we annealed antisense (as) RNA oligonucleotides to a ^{32}P-cap labeled 75 nt nonstructured target RNA (Figure 2A). Duplex formation restricts the accessibility of the target site, whereby all asRNA oligonucleotides bind with a similar stability of ΔG ≥ −30 kcal/mol to the target RNA. An asRNA, blocking the complete target site was used as a negative control (Figure 2A; full). The differentially blocked target RNAs were subjected to in vitro cleavage reactions using affinity-purified human RISC. Under single turnover conditions (Figures 2B–2D), blocking of significant parts of the target sequence resulted in severe impairments of cleavage, both in the 5′- and the 3′ parts (Figures 2B–2D; BL11-21, BL13-21, BL1-10, and BL1-8, respectively). Interestingly, blocking 6 nt or 3 nt of the 21 nt target sequence in the region annealing to the 3′ part of the siRNA had no effect on

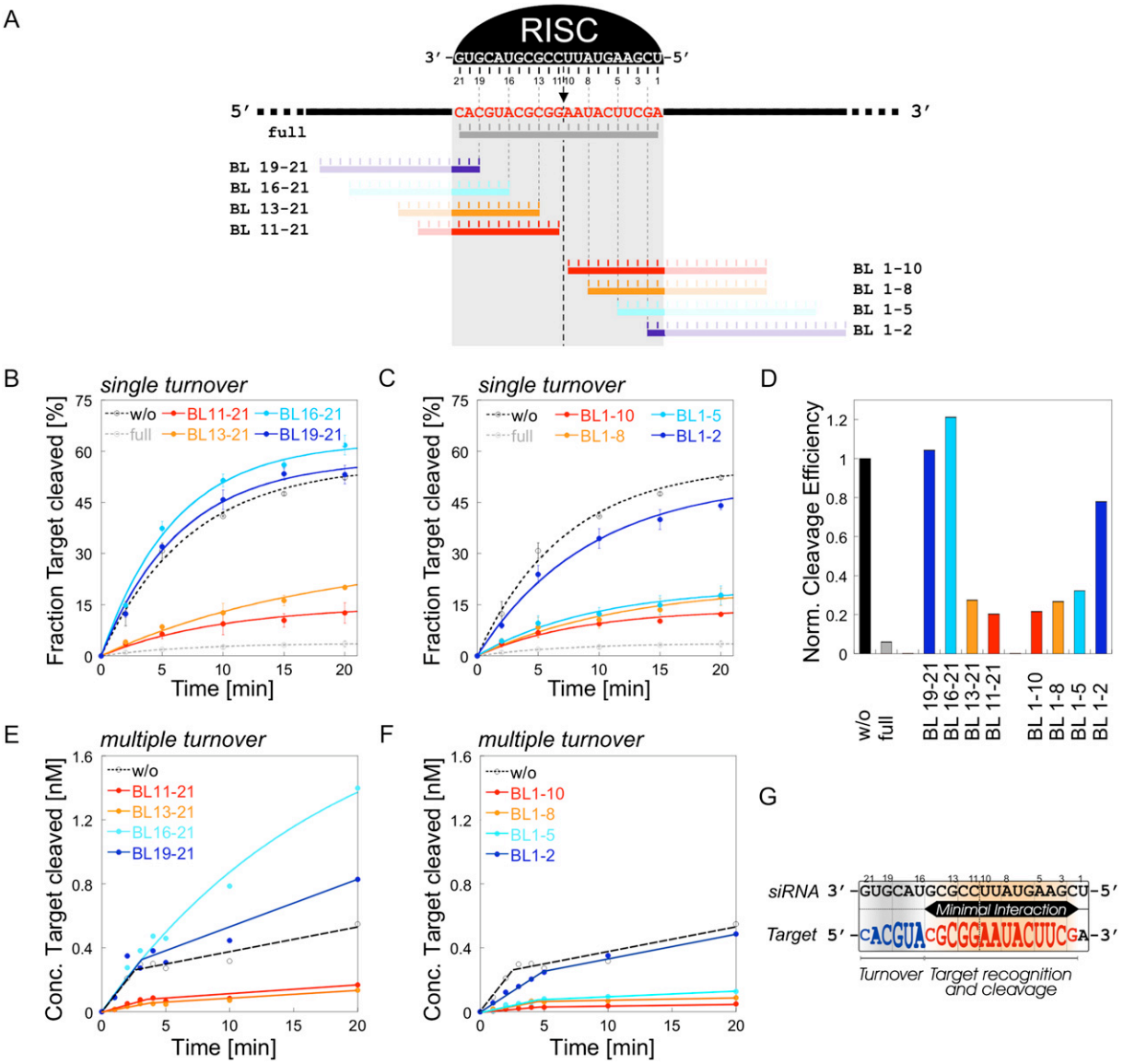

Figure 2. Partial Blocking of Target Site Accessibility Influences RISC-Mediated Target Cleavage and Multiple Turnover

(A) The 21 nt target site within an unstructured target RNA is partially blocked by the annealing of different antisense (as) RNAs to the target RNA. All asRNAs bind with a similar ΔG of ≥ -30 kcal/mol.

(B and C) Quantification of the in vitro cleavage assay under single turnover conditions, using affinity-purified RISC and the target RNAs depicted in (A). Data are represented as mean ± SD

(D) The normalized cleavage efficiency represents the initial velocity of the cleavage reaction depicted in (B) and (C). Cleavage efficiency was normalized to the positive control (w/o), which was set as 1.

(E and F) Quantification of the in vitro cleavage assay under multiple turnover conditions, using affinity-purified RISC and excess of target RNA. Data are represented as mean ± SD

(G) Schematic overview of siRNA-target RNA interactions required for efficient target recognition and cleavage or multiple turnover.

cleavage rates (Figures 2B and 2D; BL16-21 and BL19-21). In contrast, blocking 5 nt of the target site in the region annealing to the 5′ part of the siRNA (Figures 2C and 2D; BL1-5) severely impaired cleavage and even blocking only 2 nt did not fully restore cleavage rates (Figures 2C and 2D; BL1-2).

As RISC can catalyze multiple rounds of cleavage (Hutvagner and Zamore, 2002), we asked how cleavage would be affected under multiple turnover conditions. When a fully accessible target RNA is in large excess over affinity-purified human RISC, we observed a burst of cleaved product early in the time course, which was followed by

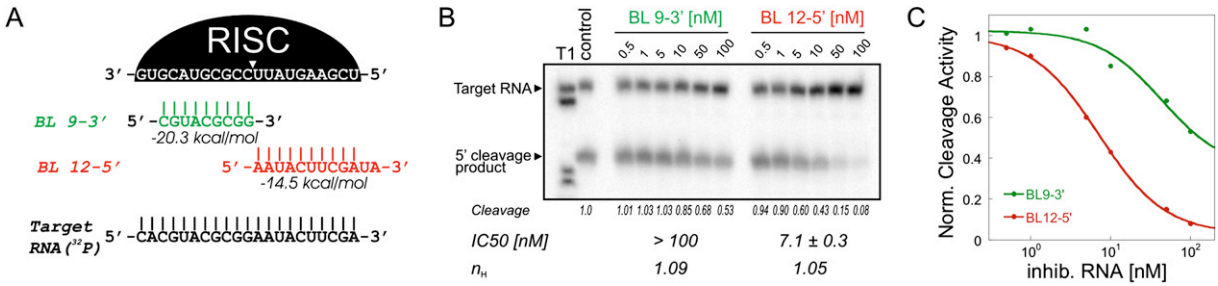

Figure 3. The siRNA 5′ and 3′ Parts Have Differential Binding Capabilities

(A) Affinity-purified RISC was preincubated with different concentrations of short RNAs directed against the 5′- or the 3′ parts of the siRNA. The free energy value (ΔG) for both duplexes is indicated. Subsequently, a 21 nt ^{32}P-labeled target RNA was added, the reaction was further incubated and cleavage was analyzed.

(B and C) Representative in vitro cleavage reaction. Fraction of target cleaved was quantified and normalized to the positive control (w/o as RNA). The concentration of inhibitory RNA required for half-maximal inhibition (IC_{50}), as well as the approximate amount of inhibitory RNA binding to one RISC enzyme (Hill coefficient, n_H) is indicated.

a slower rate of cleavage (Figures 2E and 2F, w/o). We concluded that the initial phase of the reaction corresponded to a single turnover of enzyme and the markedly slower second phase represented the steady state increase in product, which is most probably limited by product release (Haley and Zamore, 2004). The rate of cleavage was similar, both in the presence or absence of ATP (Figure S2), suggesting that an auxiliary factor that might facilitate substrate release (Haley and Zamore, 2004), is absent in affinity-purified human RISC. When significant parts of the target site were blocked under multiple turnover conditions, we observed strong inhibition of both reaction phases, similar to what we detected under single turnover conditions (Figures 2E and 2F; BL11-21, BL13-21, BL1-10, and BL1-8). The effect was likewise severe after blocking 5 nt of the target site in the region annealing to the 5′ part of the siRNA and could still be observed when blocking was restricted to 2 nt (Figure 2F; BL1-5 and BL1-2). Remarkably, blocking 6 nt of the target site in the region annealing to the 3′ part of the siRNA, led to a strong increase in steady state product formation, whereas the presteady state increase remained unaltered compared to the positive control (Figure 2E; BL16-21 and w/o). A less pronounced, but still detectable effect on steady state product increase was observed when only 3 nt of the 5′-target site were blocked (Figure 2E; BL19-21). These data indicate that efficient target recognition and cleavage requires the annealing of nt 2-15 of the siRNA, whereas impairing the annealing of the siRNA 3′ part to the target site (nt 16-21) facilitates multiple turnover (Figure 2G). It also demonstrates an asymmetrical function of siRNAs with the 5′ part being essential for the initial target recognition and the 3′ part contributing to the stability of siRNA-target RNA association, therefore affecting multiple turnover. Our data is furthermore consistent with the notion that annealing of the central part of the siRNA to the target is a quality control step for RISC-mediated cleavage, as it provides a catalytically permissive geometry at the active site (Haley and Zamore, 2004).

Differential Binding Capabilities of the siRNA within RISC

Why is the 5′ part of the siRNA (often referred to as the 'seed-region') so important for the process of target recognition? One could envision that the 5′ part of the siRNA within RISC is favorably structured to undergo base pairing, whereas the arrangement of the 3′ part antagonizes base pairing with the target RNA (Filipowicz, 2005; Tomari and Zamore, 2005). To test this hypothesis, we used short RNA oligonucleotides to block either the 5′ (BL 12-5′) or the 3′ part (BL 9-3′) of the siRNA component of RISC (Figure 3A). In both cases the degree of blocking extended up to the cleavage site, which, when applied to the target site, severely impaired cleavage (Figure 2). After preincubation of different concentrations of short blocking RNAs (BL 12-5′ or BL 9-3′) with RISC, a 21 nt, 5′-radiolabeled target RNA was added and the reaction was continued before cleavage was analyzed (Figure 3B). Quantification revealed that the IC_{50} value for BL 12-5′ is more than one order of magnitude lower compared to BL 9-3′ (Figure 3C), even though the free energy value for duplex formation in the case of BL 9-3′ (ΔG = −20.3 kcal/mol) is significantly higher compared to BL 12-5′ (ΔG = −14.5 kcal/mol). In both cases the data fit well to sigmoidal curves with a Hill coefficient (n_H) of around 1 (Figure 3B), consistent with a sequence specific inhibition of RISC in a 1:1 stoichiometry. This shows that, when organized in RISC, the 3′ part of the siRNA can undergo base pairing much less efficiently than the 5′ part.

Minimal RISC Exhibits Annealing Activity

Very little is known about how RISC efficiently finds target sequences. To address this question we determined the cleavage rate of a 21 nt target RNA in vitro, using affinity-purified human RISC, and compared it to the rate of annealing of the same siRNA to the same target in the absence of RISC under identical experimental conditions. We found that target cleavage by RISC is 9-fold faster (k_{obs} = 0.09 ± 0.005 min^{-1}) than the formation of an RNA

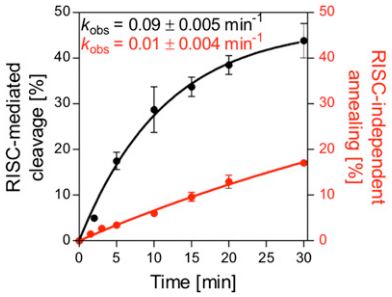

Figure 4. RISC Promotes siRNA-Target RNA Hybridization

The cleavage rate of a 21 nt substrate was compared to the annealing rate of the same siRNA to the same target in the absence of RISC under identical experimental conditions. Quantification of the in vitro cleavage reaction (black) or annealing reaction (red) is shown. The observed rate (k_{obs}) for both reactions is indicated. Data are represented as mean ± SD

duplex in the absence of RISC (k_{obs} = 0.01 ± 0.004 min^{-1}) (Figure 4). The fact that, in the course of RISC-mediated cleavage, catalysis is not rate-limiting, suggests that any acceleration of cleavage rates is a result of facilitated siRNA-target association (Supplemental Text and Figure S3). Therefore, RISC seems to have an intrinsic activity which promotes the annealing of the incorporated siRNA to complementary sequences.

The Structure of Target RNAs Contribute to RISC-Mediated Target Recognition and Cleavage

To further elucidate the process of RISC-mediated target recognition we analyzed cleavage rates of target RNAs in vitro with different secondary structures but similar accessibility of the target site (Figures 5A, 5C, and 5E). We found that the presence of a single-stranded region upstream of the target site improved RISC-mediated cleavage (Open 5′; Figure 5B), leading to a more than 20-fold increase in cleavage rates (k_{obs} = 0.22 ± 0.009 min^{-1}; Figure S4) when compared to the annealing reaction in the absence of RISC (k_{obs} = 0.01 ± 0.003 min^{-1}; Figure S4). Interestingly, when the single-stranded region was replaced by a stem-loop structure, cleavage rates dropped to a level which was very similar to the one of the 21nt target site alone, suggesting that single-stranded but not double-stranded regions within target RNAs can further improve target cleavage by RISC. We obtained similar results by analyzing cleavage rates of target RNAs with identical structures downstream of the target site (Figure S5), which, together with the fact that no energy from ATP or GTP is required for this process (Figure S6), argues against a model in which RISC by itself might directionally scan along target RNAs to find complementary sequences. Additionally, cleavage rates are not influenced by the presence or absence of a 5′-cap (Figure S7), although it is thought to be an important functional feature of target RNAs in respect to RISC-mediated translational repression (Humphreys et al., 2005; Pillai et al., 2005; Wang et al., 2006).

It has already been speculated that the flanking sequences of a target RNA might facilitate target recognition by RISC in *Drosophila*, as it was shown that the specific inhibition of miRNAs, using antisense 2′-O-methyl oligonucleotides, is more efficient in case of 31 mers compared to 21 mers (Hutvagner et al., 2004). To verify the potential influence of an increasing single-stranded character of target RNAs on RISC-mediated target recognition, we designed substrates with single-stranded regions surrounding the target site (Figure 5C, Open/Open) and compared cleavage rates in vitro to target RNAs in which these single-stranded regions form a stem, rendering the target site accessible in a 31 nt, 41 nt, or 51 nt loop (Figure 5C, Loop 5/5, Loop 10/10, and Loop 15/15). An increase in single-stranded character of the target RNA correlated with an increase in the initial velocity of target cleavage (Figure 5D), supporting the idea that target RNA structures not involving the target site play an important role in RISC-mediated target recognition. Furthermore, the small size of the target site containing loop, especially in the case of 'Loop 5/5′ (Figures 5C and 5D), might cause a steric problem in the formation of a cleavage competent enzyme-substrate complex. In this case, target recognition might occur fast, whereas the subsequent winding of the siRNA 3′ part around the target or vice versa might be topologically difficult, therefore resulting in reduced cleavage rates.

We determined the kinetic parameters for RISC-mediated cleavage, using a target RNA with single-stranded regions upstream and downstream of the target site (Open/Open) and compared them to the same target RNA when annealed to RNA oligonucleotides upstream and downstream of the target site (Figure 5E). We observed an almost four fold increase in V_{max} in the presence of single-stranded regions surrounding the target site (Figure 5G). However, the affinity of RISC to the target site remained unaffected, as the K_M was similar within error (Figure 5G), which evidences that double-stranded regions surrounding a target site do not interfere sterically with target recognition. Moreover, if the K_d of RISC bound to its target RNA is essentially its K_M (0.65 - 0.88 nM; Figure 5G), then the free energy ($\Delta G^0 = -RT \ln K_d$) of the RISC-target interaction is about −12 kcal/mol (Haley and Zamore, 2004). This value is far smaller than the ΔG of a 21nt duplex (ΔG = −38.8 kcal/mol) and rather similar to the −9.9 kcal/mol of the siRNA nucleotides 2-8 (the 5′-seed region) bound to a perfectly complementary RNA, as determined by UV-melting analysis (Figure S8). Similar observations have been reported in a different study for a let-7-programmed RISC in *Drosophila* (Haley and Zamore, 2004). Together with the observation that the 5′ part of the siRNA within RISC is favorably structured to initiate base pairing (Figure 3) this suggests that, energetically, the decision over either target cleavage or dissociation is made without contribution of the siRNA 3′-nts, which only provide binding energy after annealing of the 5′-nts (Figure 2). On the other hand, binding energy derived from 3′-nts would

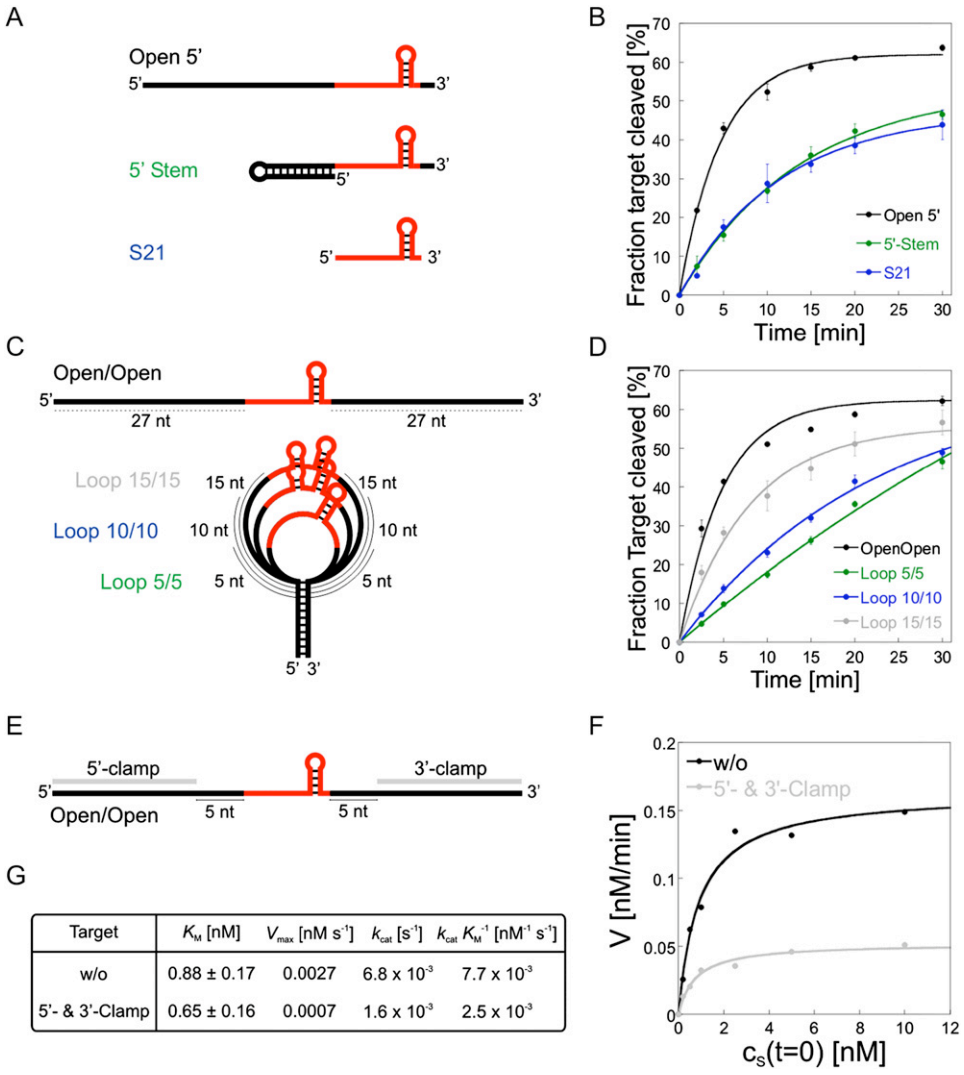

Target	K_M [nM]	V_{max} [nM s^{-1}]	k_{cat} [s^{-1}]	k_{cat} K_M^{-1} [nM^{-1} s^{-1}]
w/o	0.88 ± 0.17	0.0027	6.8×10^{-3}	7.7×10^{-3}
5'- & 3'-Clamp	0.65 ± 0.16	0.0007	1.6×10^{-3}	2.5×10^{-3}

Figure 5. The Structure of Target RNAs Contribute to RISC-Mediated Target Recognition and Cleavage

(A, C, and E) Schematic overview of target RNAs used to analyze the influence of target RNA structures that do not block target site accessibility. For further specification see text. (B and D) Quantification of the in vitro cleavage reaction using affinity-purified RISC and the indicated target RNAs. Data are represented as mean ± SD (F) RISC-mediated product formation was monitored at early time points and at different substrate concentrations using the target RNAs depicted in (E). The initial velocity of product formation (V) is plotted versus initial substrate concentration (c_S). (G) Kinetic parameters for the data sets depicted in (F) were determined from the Michaelis-Menten equation.

be necessary to confer stability to an si/miRNA-target-complex in case of noncleavable targets, like the majority of miRNA targets in animals.

RISC Has a Sequence-Independent Affinity for Single-Stranded but Not for Double-Stranded RNA

If efficient target recognition by RISC is based on its intrinsic affinity for single-stranded RNA then one would predict that RISC should be able to contact single-stranded RNA nonspecifically in the course of target recognition. To test this hypothesis we performed crosslinking experiments using 4-thiouridine (4-SU)-modified target RNAs and affinity-purified human RISC (Figures 6A and 6C). Using this approach we detected a single crosslinking band when the 4-SU-modification was located within the target site (Figure 4B, LUC Open 4-SU-39). This band migrated between 100 and 150 kDa, corresponding to the size of siRNA-loaded human Argonaute together with the target RNA. When the 4-SU modification was positioned outside this region (LUC Open 4-SU-7) we could still detect a crosslinking event, although weaker, which would be expected in case of a transient interaction. This indicates that, in the course of target recognition, RISC contacts not only the specific target site but also distant parts in a single-stranded RNA molecule. However, as the 4-SU

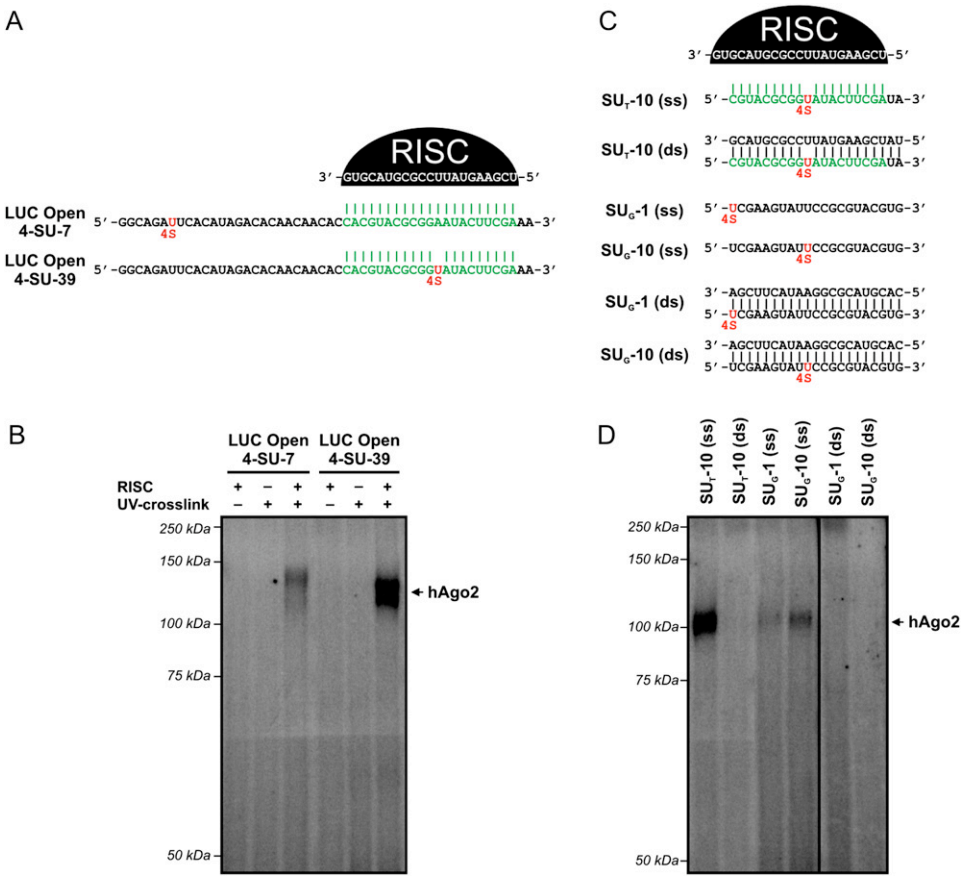

Figure 6. RISC Interacts Nonspecifically with Single-Stranded but Not with Double-Stranded RNA

(A) A single 4-thiouridine (4-SU) modification (shown in red) was introduced into the target RNA, either within the region of specific interaction with RISC (LUC Open 4-SU-39, region of specific interaction is shown in green), or outside of this region (LUC Open 4-SU-7). (B and D) Affinity-purified RISC was incubated with the indicated 4-SU-modified oligonucleotides followed by UV-irradiation. Crosslinking was analyzed by SDS-PAGE. The expected size of hAgo2 is indicated. (C) Single 4-SU-modifications (shown in red) were introduced into 21 nt RNAs that either specifically interact with the siRNA in RISC (SU$_T$-10, region of interaction is shown in green) or that have the identical sequence composition as the siRNA within RISC (SU$_G$-1 ss or SU$_G$-10 ss). Blunt-end duplexes were generated by annealing of complementary RNAs.

modification in LUC Open 4-SU-7 is close to the target site (20 nt) we cannot rule out that crosslinking might result from the close proximity of RISC after annealing to the target sequence. To exclude this possibility we used short 4-SU-modified RNAs which were either complementary to the guide strand in RISC (SU$_T$-10), or had the same sequence composition as the guide strand (SU$_G$-1 and SU$_G$-10) and therefore did not form a stable interaction with the siRNA in RISC (Figure 6C). It is important to note that affinity-purified RISC cannot be re-loaded with ss or ds siRNAs (Martinez et al., 2002), excluding the possibility that the short 4-SU-RNAs are incorporated into affinity-purified RISC as described for recombinant hAgo2 (Rivas et al., 2005). Crosslinking of Argonaute to both SU$_G$-1 and SU$_G$-10 was detected when the oligonucleotides were single-stranded, although the intensity of the crosslinking band was clearly reduced compared to the control SU$_T$-10 (Figure 6D), similar to results in Figure 6B. In all cases crosslinking could not be detected when the 4-SU-oligos were in a double-stranded conformation. Taken together, these data indicate that RISC can interact with single-stranded RNA, independently of siRNA-complementarity, but not with double-stranded RNA, which is in agreement with the observation that dsRNA is a poor target for RISC-mediated cleavage (Figure 1). The fact that this interaction seems to be highly transient, as only a large excess of single-stranded competitor RNA can slow down the rate of cleavage (Figure S9), suggests that RISC can sense high target site accessibility without losing some of its substrate specificity and cleavage efficiency. RISC might even adopt this affinity to facilitate the process of target recognition, thereby increasing enzymatic efficiency. Future studies will be needed to determine if the nonspecific single-stranded RNA binding properties of RISC relies mainly on protein-RNA or rather on nonproductive siRNA-target RNA interactions and if RISC can contact multiple RNAs simultaneously to facilitate target finding.

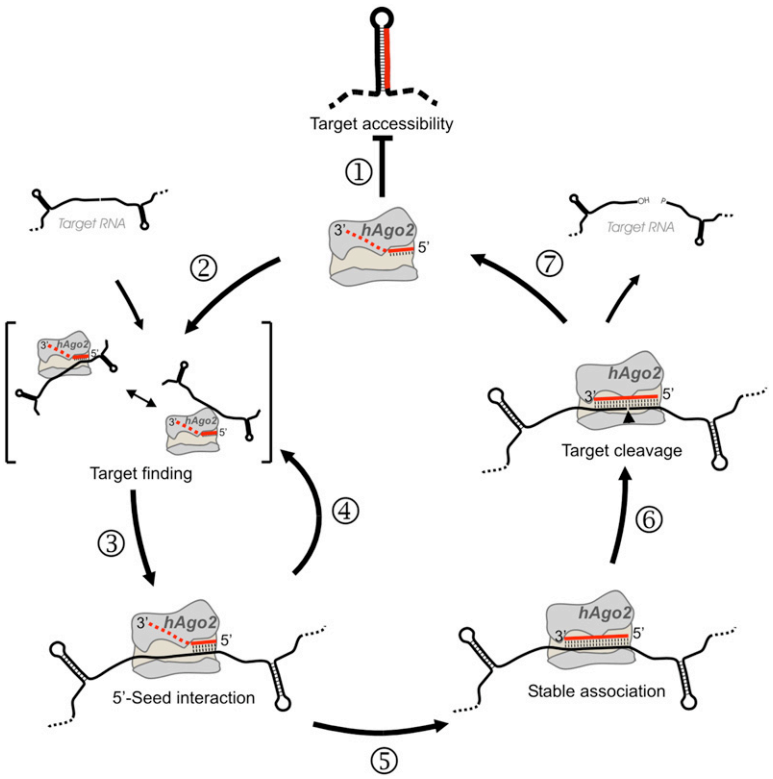

Figure 7. Model for Human RISC-Mediated Target Recognition and Cleavage

(1) RISC-mediated target recognition and cleavage is limited by the accessibility of the substrate.

(2) RISC interacts nonspecifically and transiently with single-stranded RNA and promotes the annealing of siRNA and target RNA.

(3) The initial specific RISC-target association is primarily mediated via the 5′ part of the siRNA, whereas annealing of the 3′ part is disfavored.

(4) Thermodynamically unfavorable association, as caused by 5′-seed mismatches or inaccessibility, leads to immediate dissociation of RISC.

(5) Stable association results in siRNA 3′ part annealing.

(6) In case of a high degree of complementarity and accessibility, target cleavage occurs.

(7) Target release is rate limiting for multiple rounds of cleavage and might be facilitated by auxiliary factors.

DISCUSSION

We propose the following model for human RISC-mediated target recognition and cleavage (Figure 7). (1) The accessibility of the RNA substrate clearly limits cleavage by RISC, as RISC has no activity to unfold RNA secondary structures. (2) In the course of target finding, RISC contacts nonspecifically single-stranded but not double-stranded RNA, which is in agreement with single-stranded RNA being the preferred target for RISC. Such a nonspecific affinity might even facilitate the process of target finding by bringing potential target sequences in close proximity to be tested for base pairing with the siRNA. In any case, RISC exhibits annealing activity which promotes siRNA-target RNA interactions and therefore renders nucleic-acid hybridization more efficient compared to the annealing of a single-stranded siRNA to a target in the absence of hAgo2. This activity might rely on both, the siRNA-organization - with an helical geometry of the 5′-region favoring duplex formation - or a nonspecific affinity of RISC toward RNA substrates which might relate to the overall basicity of hAgo proteins. Interestingly, similar observations have been reported for the Sm-like protein Hfq, which mediates small RNA-mRNA interactions in bacteria, suggesting that facilitated nucleic acid hybridization is a common strategy to increase the efficiency of small RNA-mediated regulatory processes within the cell (Moller et al., 2002; Wassarman, 2002; Zhang et al., 2002). (3) The specific interaction between RISC and the substrate is initiated via the 5′ part of the siRNA, as the 3′ part is less favorably structured to undergo base pairing before the initial recognition of a target. In this regard, our results support a so called ‘‘two-state model’’ for RISC-mediated target recognition (Filipowicz, 2005; Tomari and Zamore, 2005). In an initial ‘‘double-anchor state’’ the siRNA 5′-end is tethered to the PIWI domain and the 3′-end to the PAZ domain of hAgo2. In this state the 5′ part of the siRNA is exposed to the solvent in a semi-helical conformation, as supported by structural data derived from bacterial Argonaute homologs (Yuan et al., 2005). By contrast, the siRNA 3′ part is organized in a way that antagonizes base pairing to the target. This might explain why binding of the siRNA 3′ part to a complementary RNA is offset by the loss of RNA-protein binding energy. Alternatively, the siRNA 3′ part bound to the PAZ domain might be less accessible for base pairing, and accessibility would increase only after rearrangement of the siRNA, following the initial recognition via the siRNA 5′ part. In any case, the outcome would be a reduction in the stability of initial siRNA-substrate interactions to a level in which even single nucleotide mismatches or a minor target-inaccessibility could result in loss of interaction and therefore block any further RNAi effector step (4). This model also agrees with previous results showing that the 5′-nts of siRNAs and miRNAs contribute more to target binding than the 3′-nts, as determined by mutational analysis, and that even minor changes in the thermodynamic stability of the 5′-seed region can impair cleavage (Doench and

Sharp, 2004; Haley and Zamore, 2004; Schwarz et al., 2006). It could additionally explain how only slight changes in the siRNA sequence can lead to major differences in RNAi efficiency as the nucleotide composition of the seed region would determine the absolute level of such a thermodynamic threshold (Boese et al., 2005). By contrast, the identification of 3′-compensatory miRNA target sites, which show insufficient 5′-seed binding but require strong 3′ binding, together with the recent observation that perfect seed pairing is not a generally reliable predictor for miRNA-target interactions argues against such a thermodynamic threshold model (Brennecke et al., 2005; Didiano and Hobert, 2006). A possible explanation for this discrepancy could rely in that miRISC-mediated target recognition might, at least in some cases, differ from the one of siRISC. It is known that in humans only hAgo2 can mediate target cleavage, in contrast to the three other Argonaute proteins (hAgo1, 3 and 4), although all of them are functional in mediating translational repression when artificially tethered to mRNAs (Meister et al., 2004; Pillai et al., 2004). As all hAgo proteins were found to be associated with siRNAs and miRNAs (Liu et al., 2004; Meister et al., 2004), it might likely be that different Argonaute-si/miRNA complexes differ from each other in how the guide-RNAs are exposed, directing different Argonaute complexes to distinct target sites, possibly even by using varying regions of the identical si/miRNA. Therefore the degree of complementarity between si/miRNAs and their targets would dictate the regulatory outcome. Alternatively, miRISC might be supported by additional *cis*-regulatory factors, which stabilize an energetically unfavorable miRISC-target RNA interaction in vivo. (5) In case of a stable association to the 5′-seed, the siRNA 3′ part anneals to the target. Base pairing of this 3′ part is disfavored either energetically or structurally to avoid nonproductive interactions, which would slow down the enzymatic reaction. (6) As a result of a continuous A-form helix around the cleavage site, cleavage occurs. (7) Multiple rounds of cleavage are limited by the release of the cleaved target from the siRNA, which in vivo might be facilitated in the presence of ATP by an auxiliary factor that remains to be identified.

EXPERIMENTAL PROCEDURES

General Methods

For generation of target RNAs, antisense DNA oligonucleotides (Sigma-Genosys; Table S1) were annealed to a T7 promoter sense oligonucleotide (pT7 fwd; Table S1) and subjected to in vitro transcription reactions using MEGAshortscript transcription kit (Ambion) or RNAMaxx high yield transcription kit (Stratagene) according to the instructions of the manufacturers, followed by PAGE purification. Transcribed target RNAs were Cap-labeled as described previously (Martinez et al., 2002).

Blocking (BL- and Clamp-) RNAs, as well as 21 nt target RNA (S21), siRNA and 4-thiouridine-RNAs (Table S2) were chemically synthesized (Dharmacon), deprotected according to the manufacturers' protocol and resolved in water. Chemically synthesized target RNAs were labeled using 10 pmol RNA, 10 pmol γ-^{32}P-ATP (Hartmann Analytic, 3000 Ci/mmol) and T4 polynucleotide kinase (New England Biolabs) according to the instructions of the manufacturer, followed by PAGE purification.

Affinity Purification of RISC

RISC was affinity-purified as previously described using an siRNA duplex containing biotin at both of its 3′ ends (Martinez et al., 2002; Martinez and Tuschl, 2004).

Target RNA Cleavage Assay

Cleavage assays were essentially performed as described (Martinez and Tuschl, 2004). Target RNAs were refolded at a final concentration of 1 nM in water by heat treatment for 5 min at 95°C and slowly cooling to room temperature to assure proper folding. For target RNA duplex formation, annealing reactions were performed using 50 nM target RNA and 100 nM antisense RNA in 10× Lysis buffer (30 mM HEPES [pH 7.4], 100 mM KCl, 2 mM $MgCl_2$). Duplex formation was controlled on a 10% native PAA gel. Cleavage assays were performed using 0.2 nM target RNA for single turnover conditions and 5 nM for multiple turnover conditions at 30°C except for Figure 1B where cleavage was analyzed at 42°C. Aliquots were withdrawn at the indicated time points, the reaction was stopped by the addition of 5 volumes of urea-stop solution, heat treated for 2 min at 90°C and loaded on a denaturing PAA gel. The fact that cleavage reactions did not proceed to completion (maximum fraction of target cleaved at late time points ~80%, Figure S1) could be explained by the presence of cleavage incompetent siRNA-protein complexes constituted of catalytically inactive Argonaute proteins which compete with hAgo2 containing complexes for target binding.

For the siRNA-blocking assay, affinity-purified RISC (~0.4 nM final concentration) was incubated under conditions of a normal target RNA cleavage assay with the indicated concentration of blocking RNAs at 25°C. After 1 hr a 21-nt 5′-radiolabeled target RNA (S21) was added to a final concentration of 0.2 nM. The cleavage reaction was continued at 25°C for 1 hr and the reaction was stopped by adding 1.5 volumes of urea stop solution.

General data analysis and kinetic analysis was performed as described in Supplemental Experimental Procedures.

Cell Culture and Transient Transfection

siRNAs used in transient transfection experiments had identical sequences than the duplex used for affinity purification of human RISC (Table S2). siRNA-duplexes were annealed to a final concentration of 10 μM in 10× Lysis buffer. HeLa cells were cultured in 24-well plates and transfected with the indicated amount of siRNA, 0.2 μg of the indicated phRL-reporter and 0.1 μg *lacZ* expression vector pUHC 16-1 for internal standardisation (Ameres et al., 2005) using Lipofectamine 2000 (Invitrogen) according to the instructions of the manufacturer. 24 h post transfection luciferase activity was determined using Renilla luciferase assay system (Promega) and β-Galactosidase activity was determined as described previously (Ameres et al., 2005). Luciferase activity was normalized to transfection efficiency and protein levels. Normalized luciferase activity after transfection of plasmids without siRNA was set as 1. Values represent the mean of triplicates. Data analysis was performed as described in Supplemental Experimental Procedures.

Strand Annealing Assay

0.4 nM of the siRNA guide strand was incubated with 0.2 nM 5′-radiolabeled 21-nt target RNA (Table S2) under identical conditions as described for target RNA cleavage assays, whereby RISC was replaced by buffer B (30 mM HEPES [pH 7.4], 100 mM KCl, 5 mM $MgCl_2$, 0.5 mM DTT, 3% Glycerol). The reaction was performed at 30°C. Aliquots were withdrawn at the indicated time points; the reaction was stopped by the addition of 1 volume of stop solution (10% glycerol, 150 mM EDTA, 2% SDS and 400 nM nonlabeled target RNA) and loaded on a 10% native PAA gel. Data analysis was performed as described in Supplemental Experimental Procedures.

Crosslinking Reactions

Crosslinking reactions were performed as described for target RNA cleavage reactions using 10 nM 5′-radiolabeled 4-thiouridine-RNAs (Table S2). Duplex formation was performed in 10 x Lysis buffer using 100 nM 5′-radiolabeled 4-thiouridine RNA and 200 nM nonlabeled antisense RNA (for sequences see Table S2). Reactions were incubated in 96-well plates on ice and irradiated at 1 cm distance for 10 min at 365 nm UV light. Crosslinks were resolved on an 8% SDS-PAA gel and analyzed by phosphorimaging.

Supplemental Data

Supplemental Data include Supplemental Text, Supplemental Experimental Procedures, Supplemental References, three tables, and nine figures and can be found with this article online at http://www.cell.com/cgi/content/full/130/1/101/DC1/.

ACKNOWLEDGMENTS

We thank the members of the Schroeder and Martinez labs for encouragement, helpful discussions, and comments on the manuscript; N. Piganeau for helpful advices and discussions; C. Berens and W. Hillen for kindly providing plasmid pUHC16-1; K. Weinlaender for patience and discussions; and P.D. Zamore and W. Filipowicz for critically reading the manuscript. S.L.A. is funded by the Austrian Science Fund FWF through WK001. J.M. is a Junior Group Leader at IMBA, the Institute of Molecular Biotechnology supported by the Austrian Academy of Sciences. R.S. is funded by the Austrian Science Fund FWF grant Z-72.

Received: November 15, 2006
Revised: March 14, 2007
Accepted: April 24, 2007
Published: July 12, 2007

REFERENCES

Ameres, S.L., Drueppel, L., Pfleiderer, K., Schmidt, A., Hillen, W., and Berens, C. (2005). Inducible DNA-loop formation blocks transcriptional activation by an SV40 enhancer. EMBO J. *24*, 358–367.

Bernstein, E., Caudy, A.A., Hammond, S.M., and Hannon, G.J. (2001). Role for a bidentate ribonuclease in the initiation step of RNA interference. Nature *409*, 363–366.

Boese, Q., Leake, D., Reynolds, A., Read, S., Scaringe, S.A., Marshall, W.S., and Khvorova, A. (2005). Mechanistic insights aid computational short interfering RNA design. Methods Enzymol. *392*, 73–96.

Brennecke, J., Stark, A., Russell, R.B., and Cohen, S.M. (2005). Principles of microRNA-target recognition. PLoS Biol. *3*, e85. 10.1371/journal.pbio.0030085.

Brown, K.M., Chu, C.Y., and Rana, T.M. (2005). Target accessibility dictates the potency of human RISC. Nat. Struct. Mol. Biol. *12*, 469–470.

Caudy, A.A., Ketting, R.F., Hammond, S.M., Denli, A.M., Bathoorn, A.M., Tops, B.B., Silva, J.M., Myers, M.M., Hannon, G.J., and Plasterk, R.H. (2003). A micrococcal nuclease homologue in RNAi effector complexes. Nature *425*, 411–414.

Caudy, A.A., Myers, M., Hannon, G.J., and Hammond, S.M. (2002). Fragile X-related protein and VIG associate with the RNA interference machinery. Genes Dev. *16*, 2491–2496.

Didiano, D., and Hobert, O. (2006). Perfect seed pairing is not a generally reliable predictor for miRNA-target interactions. Nat. Struct. Mol. Biol. *13*, 849–851.

Doench, J.G., and Sharp, P.A. (2004). Specificity of microRNA target selection in translational repression. Genes Dev. *18*, 504–511.

Elbashir, S.M., Harborth, J., Lendeckel, W., Yalcin, A., Weber, K., and Tuschl, T. (2001a). Duplexes of 21-nucleotide RNAs mediate RNA interference in cultured mammalian cells. Nature *411*, 494–498.

Elbashir, S.M., Lendeckel, W., and Tuschl, T. (2001b). RNA interference is mediated by 21- and 22-nucleotide RNAs. Genes Dev. *15*, 188–200.

Elbashir, S.M., Martinez, J., Patkaniowska, A., Lendeckel, W., and Tuschl, T. (2001c). Functional anatomy of siRNAs for mediating efficient RNAi in Drosophila melanogaster embryo lysate. EMBO J. *20*, 6877–6888.

Filipowicz, W. (2005). RNAi: The Nuts and Bolts of the RISC Machine. Cell *122*, 17–20.

Fire, A., Xu, S., Montgomery, M.K., Kostas, S.A., Driver, S.E., and Mello, C.C. (1998). Potent and specific genetic interference by double-stranded RNA in Caenorhabditis elegans. Nature *391*, 806–811.

Gu, S., and Rossi, J.J. (2005). Uncoupling of RNAi from active translation in mammalian cells. RNA *11*, 38–44.

Haley, B., and Zamore, P.D. (2004). Kinetic analysis of the RNAi enzyme complex. Nat. Struct. Mol. Biol. *11*, 599–606.

Hammond, S.M., Bernstein, E., Beach, D., and Hannon, G.J. (2000). An RNA-directed nuclease mediates post-transcriptional gene silencing in Drosophila cells. Nature *404*, 293–296.

Hammond, S.M., Boettcher, S., Caudy, A.A., Kobayashi, R., and Hannon, G.J. (2001). Argonaute2, a link between genetic and biochemical analyses of RNAi. Science *293*, 1146–1150.

Heale, B.S., Soifer, H.S., Bowers, C., and Rossi, J.J. (2005). siRNA target site secondary structure predictions using local stable substructures. Nucleic Acids Res. *33*, e30.

Humphreys, D.T., Westman, B.J., Martin, D.I., and Preiss, T. (2005). MicroRNAs control translation initiation by inhibiting eukaryotic initiation factor 4E/cap and poly(A) tail function. Proc. Natl. Acad. Sci. USA *102*, 16961–16966.

Hutvagner, G., Simard, M.J., Mello, C.C., and Zamore, P.D. (2004). Sequence-specific inhibition of small RNA function. PLoS Biol. *2*, e98. 10.1371/journal.pbio.0020098.

Hutvagner, G., and Zamore, P.D. (2002). A microRNA in a multiple-turnover RNAi enzyme complex. Science *297*, 2056–2060.

Ishizuka, A., Siomi, M.C., and Siomi, H. (2002). A Drosophila fragile X protein interacts with components of RNAi and ribosomal proteins. Genes Dev. *16*, 2497–2508.

Ketting, R.F., Fischer, S.E., Bernstein, E., Sijen, T., Hannon, G.J., and Plasterk, R.H. (2001). Dicer functions in RNA interference and in synthesis of small RNA involved in developmental timing in C. elegans. Genes Dev. *15*, 2654–2659.

Khvorova, A., Reynolds, A., and Jayasena, S.D. (2003). Functional siRNAs and miRNAs exhibit strand bias. Cell *115*, 209–216.

Knight, S.W., and Bass, B.L. (2001). A role for the RNase III enzyme DCR-1 in RNA interference and germ line development in Caenorhabditis elegans. Science *293*, 2269–2271.

Lee, Y., Ahn, C., Han, J., Choi, H., Kim, J., Yim, J., Lee, J., Provost, P., Radmark, O., Kim, S., and Kim, V.N. (2003). The nuclear RNase III Drosha initiates microRNA processing. Nature *425*, 415–419.

Leuschner, P.J., Ameres, S.L., Kueng, S., and Martinez, J. (2006). Cleavage of the siRNA passenger strand during RISC assembly in human cells. EMBO Rep. *7*, 314–320.

Liu, J., Carmell, M.A., Rivas, F.V., Marsden, C.G., Thomson, J.M., Song, J.J., Hammond, S.M., Joshua-Tor, L., and Hannon, G.J. (2004). Argonaute2 is the catalytic engine of mammalian RNAi. Science *305*, 1437–1441.

Long, D., Lee, R., Williams, P., Chan, C.Y., Ambros, V., and Ding, Y. (2007). Potent effect of target structure on microRNA function. Nat. Struct. Mol. Biol. *14*, 287–294.

Luo, K.Q., and Chang, D.C. (2004). The gene-silencing efficiency of siRNA is strongly dependent on the local structure of mRNA at the targeted region. Biochem. Biophys. Res. Commun. *318*, 303–310.

Ma, J.B., Yuan, Y.R., Meister, G., Pei, Y., Tuschl, T., and Patel, D.J. (2005). Structural basis for 5′-end-specific recognition of guide RNA by the A. fulgidus Piwi protein. Nature *434*, 666–670.

Martinez, J., Patkaniowska, A., Urlaub, H., Luhrmann, R., and Tuschl, T. (2002). Single-stranded antisense siRNAs guide target RNA cleavage in RNAi. Cell *110*, 563–574.

Martinez, J., and Tuschl, T. (2004). RISC is a 5′ phosphomonoester-producing RNA endonuclease. Genes Dev. *18*, 975–980.

Mathews, D.H., Sabina, J., Zuker, M., and Turner, D.H. (1999). Expanded sequence dependence of thermodynamic parameters improves prediction of RNA secondary structure. J. Mol. Biol. *288*, 911–940.

Matranga, C., Tomari, Y., Shin, C., Bartel, D.P., and Zamore, P.D. (2005). Passenger-strand cleavage facilitates assembly of siRNA into Ago2-containing RNAi enzyme complexes. Cell *123*, 607–620.

Meister, G., Landthaler, M., Patkaniowska, A., Dorsett, Y., Teng, G., and Tuschl, T. (2004). Human Argonaute2 mediates RNA cleavage targeted by miRNAs and siRNAs. Mol. Cell *15*, 185–197.

Miyoshi, K., Tsukumo, H., Nagami, T., Siomi, H., and Siomi, M.C. (2005). Slicer function of Drosophila Argonautes and its involvement in RISC formation. Genes Dev. *19*, 2837–2848.

Moller, T., Franch, T., Hojrup, P., Keene, D.R., Bachinger, H.P., Brennan, R.G., and Valentin-Hansen, P. (2002). Hfq: a bacterial Sm-like protein that mediates RNA-RNA interaction. Mol. Cell *9*, 23–30.

Napoli, C., Lemieux, C., and Jorgensen, R. (1990). Introduction of a Chimeric Chalcone Synthase Gene into Petunia Results in Reversible Co-Suppression of Homologous Genes in trans. Plant Cell *2*, 279–289.

Nykanen, A., Haley, B., and Zamore, P.D. (2001). ATP requirements and small interfering RNA structure in the RNA interference pathway. Cell *107*, 309–321.

Overhoff, M., Alken, M., Far, R.K., Lemaitre, M., Lebleu, B., Sczakiel, G., and Robbins, I. (2005). Local RNA target structure influences siRNA efficacy: a systematic global analysis. J. Mol. Biol. *348*, 871–881.

Pham, J.W., Pellino, J.L., Lee, Y.S., Carthew, R.W., and Sontheimer, E.J. (2004). A Dicer-2-dependent 80s complex cleaves targeted mRNAs during RNAi in Drosophila. Cell *117*, 83–94.

Pillai, R.S., Artus, C.G., and Filipowicz, W. (2004). Tethering of human Ago proteins to mRNA mimics the miRNA-mediated repression of protein synthesis. RNA *10*, 1518–1525.

Pillai, R.S., Bhattacharyya, S.N., Artus, C.G., Zoller, T., Cougot, N., Basyuk, E., Bertrand, E., and Filipowicz, W. (2005). Inhibition of translational initiation by Let-7 MicroRNA in human cells. Science *309*, 1573–1576.

Rand, T.A., Petersen, S., Du, F., and Wang, X. (2005). Argonaute2 cleaves the anti-guide strand of siRNA during RISC activation. Cell *123*, 621–629.

Rivas, F.V., Tolia, N.H., Song, J.J., Aragon, J.P., Liu, J., Hannon, G.J., and Joshua-Tor, L. (2005). Purified Argonaute2 and an siRNA form recombinant human RISC. Nat. Struct. Mol. Biol. *12*, 340–349.

Sasaki, T., Shiohama, A., Minoshima, S., and Shimizu, N. (2003). Identification of eight members of the Argonaute family in the human genome small star, filled. Genomics *82*, 323–330.

Schubert, S., Grunweller, A., Erdmann, V.A., and Kurreck, J. (2005). Local RNA target structure influences siRNA efficacy: systematic analysis of intentionally designed binding regions. J. Mol. Biol. *348*, 883–893.

Schwarz, D.S., Ding, H., Kennington, L., Moore, J.T., Schelter, J., Burchard, J., Linsley, P.S., Aronin, N., Xu, Z., and Zamore, P.D. (2006). Designing siRNA that distinguish between genes that differ by a single nucleotide. PLoS Genet. *2*, e140. 10.1371/journal.pgen.0020140.

Schwarz, D.S., Hutvagner, G., Du, T., Xu, Z., Aronin, N., and Zamore, P.D. (2003). Asymmetry in the assembly of the RNAi enzyme complex. Cell *115*, 199–208.

Schwarz, D.S., Tomari, Y., and Zamore, P.D. (2004). The RNA-induced silencing complex is a Mg2+-dependent endonuclease. Curr. Biol. *14*, 787–791.

Sen, G.L., Wehrman, T.S., and Blau, H.M. (2005). mRNA translation is not a prerequisite for small interfering RNA-mediated mRNA cleavage. Differentiation *73*, 287–293.

Song, J.J., Smith, S.K., Hannon, G.J., and Joshua-Tor, L. (2004). Crystal structure of Argonaute and its implications for RISC slicer activity. Science *305*, 1434–1437.

Tomari, Y., and Zamore, P.D. (2005). Perspective: machines for RNAi. Genes Dev. *19*, 517–529.

Valencia-Sanchez, M.A., Liu, J., Hannon, G.J., and Parker, R. (2006). Control of translation and mRNA degradation by miRNAs and siRNAs. Genes Dev. *20*, 515–524.

Wang, B., Love, T.M., Call, M.E., Doench, J.G., and Novina, C.D. (2006). Recapitulation of short RNA-directed translational gene silencing in vitro. Mol. Cell *22*, 553–560.

Wassarman, K.M. (2002). Small RNAs in bacteria: diverse regulators of gene expression in response to environmental changes. Cell *109*, 141–144.

Yuan, Y.R., Pei, Y., Ma, J.B., Kuryavyi, V., Zhadina, M., Meister, G., Chen, H.Y., Dauter, Z., Tuschl, T., and Patel, D.J. (2005). Crystal structure of A. aeolicus argonaute, a site-specific DNA-guided endoribonuclease, provides insights into RISC-mediated mRNA cleavage. Mol. Cell *19*, 405–419.

Zamore, P.D., Tuschl, T., Sharp, P.A., and Bartel, D.P. (2000). RNAi: double-stranded RNA directs the ATP-dependent cleavage of mRNA at 21 to 23 nucleotide intervals. Cell *101*, 25–33.

Zhang, A., Wassarman, K.M., Ortega, J., Steven, A.C., and Storz, G. (2002). The Sm-like Hfq protein increases OxyS RNA interaction with target mRNAs. Mol. Cell *9*, 11–22.

Zuker, M. (2003). Mfold web server for nucleic acid folding and hybridization prediction. Nucleic Acids Res. *31*, 3406–3415.